ECR-driven multicusp volume H^- ion source.

M. Bacal, A.A. Ivanov Jr., C. Rouillé
Laboratoire LPTP, Ecole Polytechnique, 91128 Palaiseau, France

S. Béchu, J. Pelletier
Laboratoire EPM, ENSHMG, BP 95
38402 Saint Martin d'Hères Cedex, France

ABSTRACT

We studied the negative ion current extracted from the plasma created by seven elementary ECR sources, operating at 2.45 GHz, placed in the magnetic multipole chamber "Camembert III". We varied the pressure from 1 to 4 mTorr, with a maximum power of 1 kW and studied the plasma created in this system by measuring the various plasma parameters, including the density and temperature of the negative hydrogen ions. We found that the electron temperature is optimal for negative hydrogen ion production at 9.5 cm from the ECR sources. The tantalum-covered wall surface pollution reduces the extracted negative ion current and enhances the electron current. Tantalum evaporation has a positive effect. Tests with a grid in front of the plasma electrode and with a collar are also reported.

INTRODUCTION

The main advantage of microwave-driven negative ion sources over the filament discharge ones is the absence of short life components (the filaments). Several attempts were made to use an ECR microwave discharge for negative ion production [1-7]. In these earlier works the microwaves were injected using a waveguide in a magnetized discharge chamber, where ECR took place. In some works [1-5] a magnetic filter was used to separate this "driver" chamber, containing fast electrons, from the extraction region. Recently the magnetic filter was replaced by a negatively biased grid to stop the energetic electrons and the microwaves from penetrating into the extraction region [6, 7].

In this work we installed a two-dimensional network of elementary ECR plasma sources [8] on the upper flange of the negative ion source Camembert-III [9] conserving at the same time the original multicusp confinement system of the source. We investigated the parameters of the hydrogen plasma produced in this system using probes and laser photodetachment, and the extracted negative ion and electron currents, for a total microwave power up to 1 kW. The first results with this source were reported in [10]. The findings of these first experiments (June-July 2003) can be summarized as follows:

1. A Maxwellian, low temperature, electron distribution was found, without use of additional magnetic filter.
2. A bi-Maxwellian negative ion distribution, with a lower temperature compared to the filament discharge.
3. The effect of increasing the microwave power in the range 0.5 to 1 kW is beneficial.
4. Similar dependence of extracted currents on the plasma electrode bias, to that observed with the filament discharge. A particularly low ratio $Ie/I^-=5$ was observed.
5. Important effect of magnetic multipole chamber.

In this paper we report the long-term (of the order of six months) time evolution of the negative ion density and extracted current. In the first experiments the wall was covered with tantalum, deposited in earlier filament discharge experiments. With time the wall was polluted and we found a reduction of the negative ion extracted current. Evaporation of fresh tantalum from a filament led to the recovery of negative ion characteristics.

We studied the influence of the distance (D) from the ECR sources to the plasma electrode on the extracted negative ion and the electron currents, and from the ECR sources to the probe (d) on the plasma characteristics (electron temperature and density, negative ion density n^-).

We also tested the effect of introducing a collar, with and without an additional magnetic filter. Peters [11] reported an enhancement of the negative ion current in a non-cesiated rf ion source, along with a reduction of the extracted electron current, when a collar was used. Earlier Leung *et al* [12] found a reduction of the electron current only, when the collar was added in a non-cesiated filament discharge, but also in an rf discharge.

EXPERIMENTAL SETUP

Plasma source.

We installed on the top flange of the stainless-steel chamber of Camembert III a two-dimensional network of seven elementary independent ECR plasma sources, shown in Figure 1. These sources are described by Lacoste *et al* (see Fig. 1 in [8]). Briefly, each plasma source is made of two main parts, a permanent annular magnet with azimutal symmetry around its magnetization axis, and a microwave applicator constituted by a coaxial line, parallel to the magnetization vector. The inner conductor of the coaxial line penetrates inside the annular magnet. Each magnet is completely encapsulated in a stainless steel envelope and is water-cooled. These sources operate at 2.45 GHz microwave frequency. Thus the magnetic field intensity required for the ECR condition is 875 G. The maximum microwave power acceptable by a single source is 200 W. Figure 2 in [8] shows the configuration of the magnetic field for a samarium-cobalt magnet 30 mm long, with an outer diameter of 20 mm and an inner diameter of 6 mm. The plasma is produced by the electrons accelerated in the region of ECR coupling by the microwave electric field applied via the coaxial line. The fast electrons oscillate between the two mirrors in front of the opposite poles of the magnet and drift azimuthally around the magnet. The plasma produced by the inelastic collisions of these fast electrons diffuses away from the magnet.

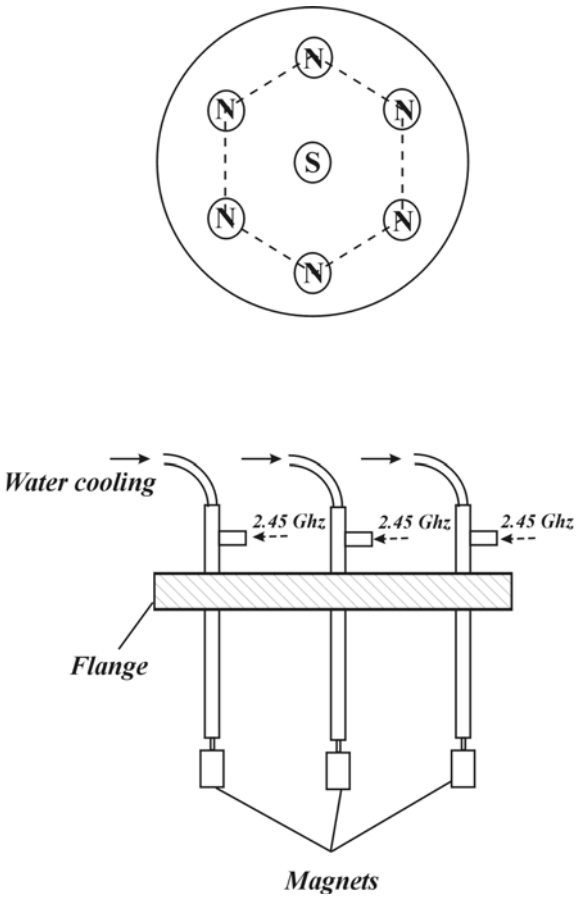

Figure 1. Top-down and side view scheme of the network of seven ECR sources implemented on the upper flange of Camembert III.

The network of seven elementary ECR sources consists of six sources with the magnets of the same magnetization, while the central source has the opposite one. This network is

operated from a single microwave power source of 1.2 kW (2.45 GHz) by dividing its microwave power into seven equal parts.

The cylindrical stainless-steel sidewall of Camembert III, described in [9] is 44 cm in diameter and 45 cm long. It contains sixteen columns of samarium-cobalt magnets with the north and south poles alternatively facing the plasma. The second end of the chamber is bounded in part by the stainless-steel plasma electrode of the extractor (10 cm in diameter), which contains an extraction hole of 0.8 cm in diameter, and in part by a water cooled annular copper plate, connected to the sidewall (which is grounded). The extractor has been described elsewhere [13]. The neighboring plasma is magnetized and due to this and to a small positive bias of the plasma electrode, large densities of volume produced negative ions concentrate in this region [13].

In the present arrangement, the source contains three distinct regions: (i) a driver region, located near the network of seven elementary ECR sources and possibly on the perimeter of the device, in the strong multicusp magnetic field); (ii) an extraction region, which extends over the central, field-free region; (iii) a weakly magnetized region with high n^-/n_e, bounded by the plasma electrode with the extraction opening. The magnetic filtering effect is provided by the magnetic field of the elementary ECR sources and possibly by the multicusp magnetic filed near the wall, which confine the fast electrons.

Diagnostics.

The plasma parameters (electron density and temperature) were measured using a microcomputer-controlled electrostatic probe (0.5 mm diam and 15 mm long) made of tungsten. The probe was located on the axis of the chamber, at a distance d from the lower end of the central elementary ECR source. The distance D between the plasma electrode and the lower end of the ECR sources was varied from 19.5 to 24.5 cm by moving the ECR sources. The probe was located at a fixed distance of 15 cm from the plasma electrode. Thus the distance (d) between the probe and the lower end of the central ECR source was varied from 4.5 cm to 9.5 cm. The H^- ion density, n-, was measured by the photodetachment technique, reviewed recently in [14]. The H^- negative ion temperature was measured using the two-laser photodetachment technique [14]. The negative ion temperature kT^- is determined from the negative ion density recovery curve after the negative ions have been destroyed by photodetachment in a small cylindrical region. The present fitting technique allows to determine the respective temperatures and fractions of the two negative ion populations [15, 16].

RESULTS

Plasma characteristics.

The electron temperature and density and the negative ion density (see Fig. 2) were measured in the pressure range from 1 to 3 mTorr for a total applied microwave power of 1 kW (*i.e.* 140 W/antenna) and for two distances from the ECR source to the probe (4.5 and 9.5 cm). Note that the electron temperature for P > 1.5 mTorr at the distance of 9.5 cm remains in the optimum range for H^- ion production, *i.e.* Te < 1 eV. Correspondingly, the negative ion density is highest for this, larger, distance. The electron density goes up linearly with hydrogen pressure and attains, at 3 mTorr and 1 kW, 3.4×10^{10} cm^{-3}.

The negative ion density also linearly increases with pressure and is not much affected by wall effects. Note that the electron temperature obtained in Camembert III is significantly lower than the one we measured in a chamber without multipolar confinement, viz. without

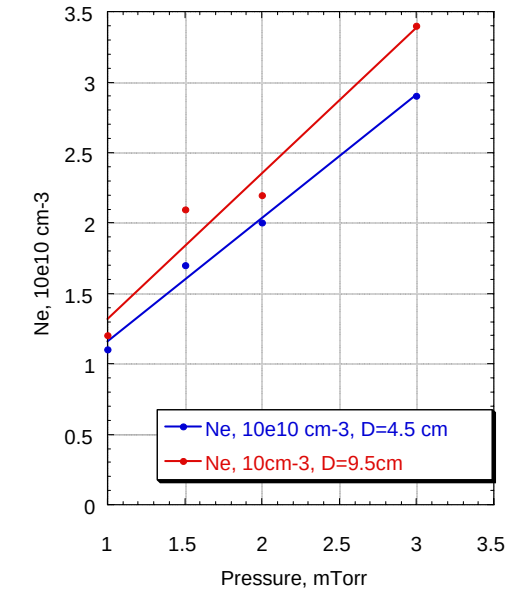

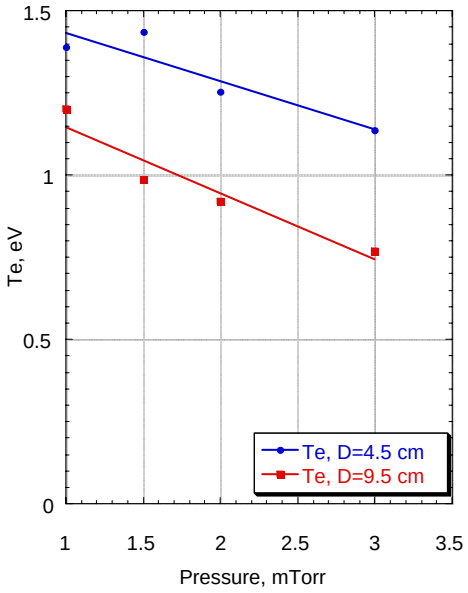

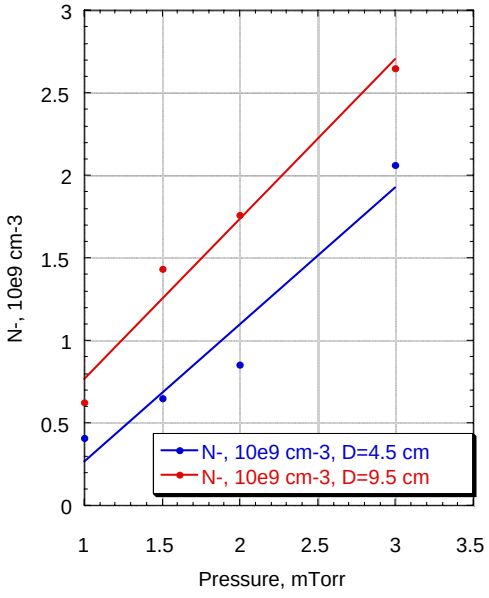

confinement it was from 1.6 eV to 2.3 eV for a pressure of 3 mTorr and power from 100 to 150 Watt/antenna. The electron density measured in Camembert III at 3 mTorr is by a factor of two higher than in the chamber without multipolar confinement, for 150 W/antenna.

The influence of multipolar confinement on plasma is discussed in details in [18]. The main multicusp magnetic field effect is the trapping of "primary" electrons – that is, the trapping in the multicusp field of the energetic electrons creating the plasma by neutral molecule ionization. The lifetime of these energetic electrons considerably increases by being trapped in magnetic field compared to field-free lifetime. The plasma itself (that is, the ions and low-temperature electrons with energies ~1eV) actually is not confined well enough by the multicusp magntic field. The increase of the plasma density due to multipolar configuration occurs essentially because of the higher ionization rate provided by an increased lifetetime of energetic electrons situated at the periphery of the chamber. The multicusp field also traps energetic electrons present in the central part of the device, several mechanisms of free electron trapping are proposed in [18]. So, the multipolar field selectively traps energetic electrons, thus the average electron energy in volume decreases.

In our system the plasma is created by ECR discharge, so the first mechanism limiting the transport of energetic electrons in volume is of the same origin as the ECR heating – the magnetic field of elementary ECR sources confines the hot electrons. The network of multipolar elementary ECR plasma sources forms an additional multicusp configuration in the chamber, and the fast electrons are formed already inside this region, so they are well confined. The energetic electrons who succeeded however to penetrate into the central, field-free part of the source, encounter the second barrier – the multicusp field of Camembert III chamber which rapidly traps these free energetic electrons. This is the reason

Figure 2. Dependence of the electron temperature, electron density and negative ion density on hydrogen pressure, for two values of the distance (d) between the central minisource and the probe.

of the observed decrease of temperature compared to the experiments with elementary ECR sources but without multicusp configuration.

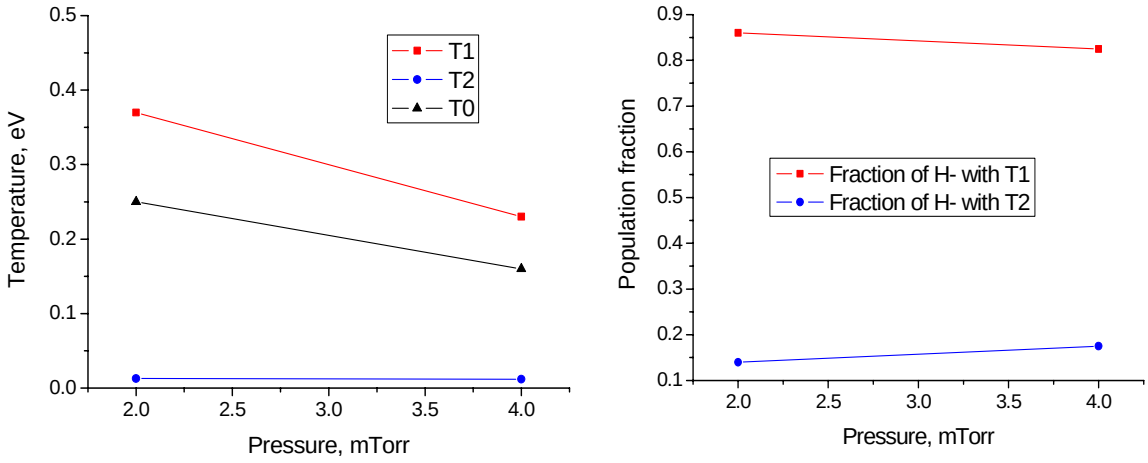

Figure 3. Dependence on hydrogen pressure of (a) negative ion temperature (average value T_0 and two values found for the two H^- populations) and (b) of population fractions.

The negative ion temperature dependence on pressure is presented in Fig. 3. We found that the negative ion population contained two groups with different temperatures. The values found for these temperatures (from the two-temperature fit) are plotted in Fig. 3 versus the hydrogen pressure for an applied power of 1 kW. The average temperature (T_0) obtained from a one-temperature fit is also shown.

The population fractions corresponding to these two temperatures, obtained from the two-temperature fit, are also shown in Fig. 3. We can note that the negative ion temperatures found here are lower than those found in a filament discharge (see Ref. 17 and 19).

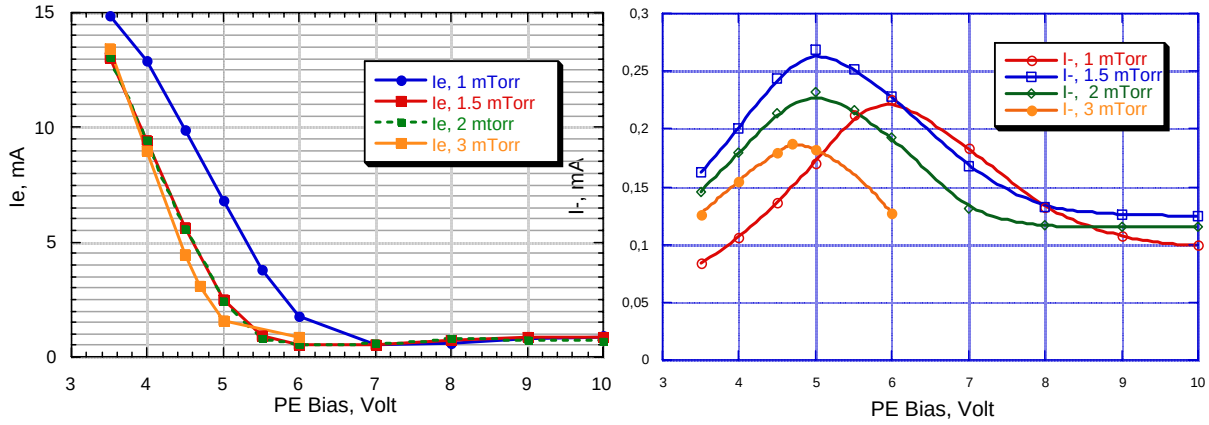

Figure 4. Effect of hydrogen pressure on the extracted negative ion and electron currents. Maximum distance between ECR sources and plasma electrode (D = 24.5 cm). Good wall conditions (72 hours after the second tantalum filament installment).

Extracted negative ion and electron currents.

The extracted negative ion and electron current dependence on the plasma electrode bias was measured for four pressures in the range 1 to 3 mTorr (see Figure 4). The results in Fig. 4 correspond to the maximum distance from the ECR sources and the plasma electrode (D=24.5 cm). The extraction and acceleration voltages were both 2 kV. The negative ion current goes

through an optimum for a plasma electrode bias, which is maximum for the lowest pressure and goes down with the pressure increase. The maximum negative ion currents are obtained for 1.5 mTorr. With D=19.5 cm the maximum negative ion current is 10% higher, as can be seen in Fig. 5, where the extracted negative ion currents are shown for these two extreme values of D studied. The optimum plasma electrode bias is lower with the larger distance D.

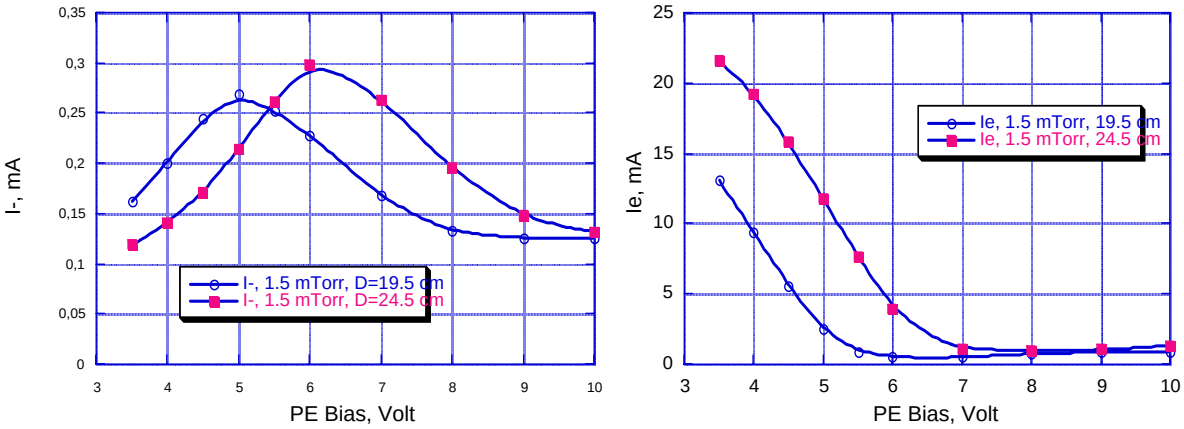

Figure 5. Effect of distance (D) from ECR minisources to the Plasma Electrode. Two distances are compared : 19.5 cm and 24.5 cm. Experiment effected under optimum pressure conditions (1.5 mTorr) with fresh tantalum deposited on the wall.

The corresponding extracted electron currents are also shown on Figures 4 and 5. Note that the extracted electron current is higher when the distance D is lower.

Effect of the wall surface state.

The study of the source during the first six months, during which there were two longer interruptions of the pumping, indicated a continuous deterioration of the source characteristics. At optimum plasma electrode bias, a reduction of the negative ion current up

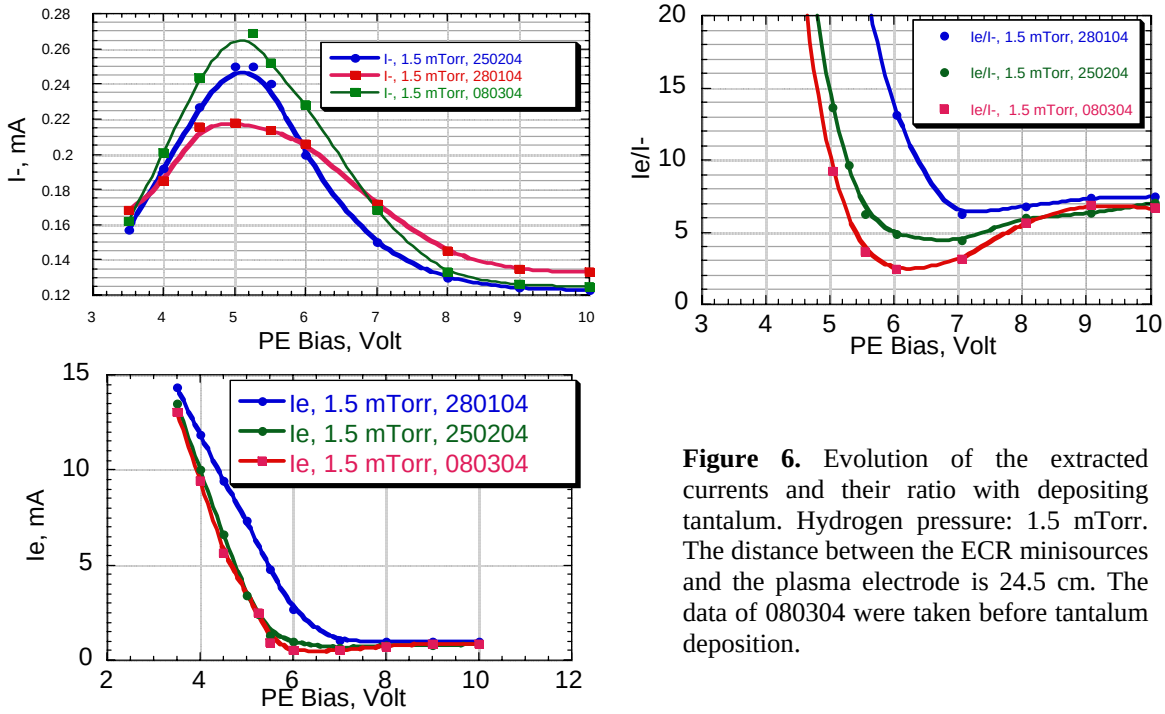

Figure 6. Evolution of the extracted currents and their ratio with depositing tantalum. Hydrogen pressure: 1.5 mTorr. The distance between the ECR minisources and the plasma electrode is 24.5 cm. The data of 080304 were taken before tantalum deposition.

to 20%, and a corresponding increase of the extracted electron current by a factor five were observed. We suspected that this change was related to the modification of the wall surface. While at the beginning of our study the wall was covered with tantalum, resulting from tantalum filament evaporation, the wall surface may have been polluted during the source operation and the interruptions of the pumping.

In order to verify this assumption, we installed a tantalum filament which could deposit tantalum on a part of the wall. Figure 6 shows the change of the extracted currents after two tantalum depositions. Note the very low ratio, $Ie/I^- = 2.5$, obtained after the second tantalum deposition for the plasma electrode bias of +6 V. These observations confirm those reported in Ref. 19 relative to the effect of tantalum deposition on the wall in a filament discharge.

Effect of a collar.

Following the positive results obtained by Peters [11] when using a collar in an rf source operated in pure hydrogen, we decided to study the effect of such a collar in our source.

We fixed the collar on the plasma electrode, which lead to a reduction of the extraction opening diameter from 8 to 7 mm. The collar potential is imposed by the plasma electrode bias. The collar is made of copper, its inner wall surface is covered with a tantalum foil. Its inner diameter is 18 mm, its inner length - 16 mm. The experiments were performed at 2 mTorr, with the distance D=24.5 cm.

As stated elsewhere [13] a weak transverse magnetic field (maximum 20 Gauss) is present in the plasma in front of the plasma electrode and is due to leak from two magnets in the extraction electrode. When the plasma electrode is biased positive this weak magnetic field leads to the increase of the negative ion density and the reduction of the electron density in front of the extraction opening. Our first experiments with the collar were effected in the presence of this weak magnetic field only, without adding any additional magnetic filter. The result is shown on Figure 7 by the red curve labeled ‘without MF’. It can be compared to the green curve with the label ‘no collar’. Note that the presence of the collar reduces the negative ion current three times, much more than the factor 49/64=0.76 due to the reduction in the extraction opening. The beneficial effect is the reduction of the electron current.

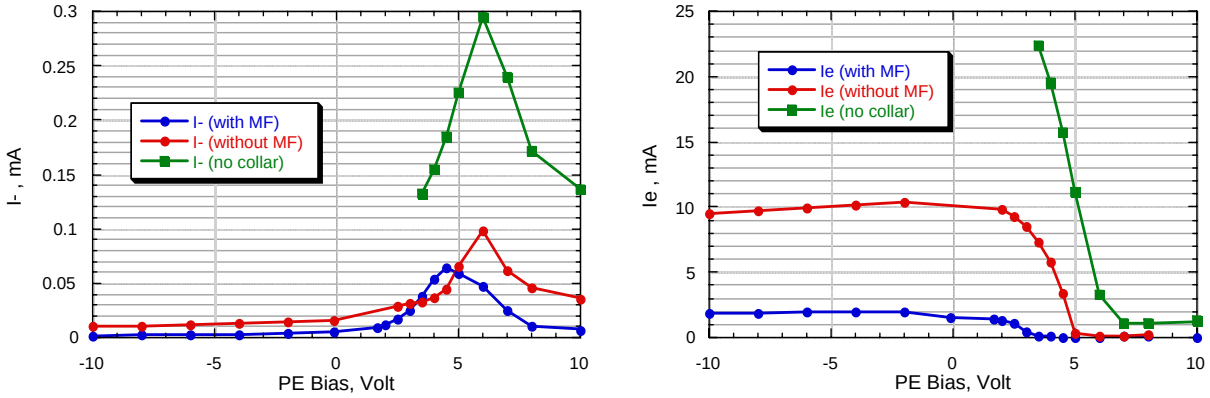

Figure 7. Illustration of the effect of introducing a collar. Hydrogen pressure 2 mTorr.

In the next experiment we introduced an additional magnetic filter produced by two small magnets, which was aligned with the existing one. The total maximum transverse field is 200 Gauss. The result is shown on Figure 7 by the violet curve labeled ‘with MF’. One can note a further reduction of the negative ion current, as well as that of the extracted electron current,

which attains values lower than 0.1 mA at optimum plasma electrode bias. The experiments were conducted at positive and negative plasma electrode bias. As can be noted from Figure 7, no enhancement of the negative ion current occurs with increasing the negative bias of the plasma electrode.

We should note that in our case the collar is introduced in a plasma region which does not contain any fast electrons, which was not the case in [11]. Our results are very similar to those reported by Leung *et al* [13] in pure hydrogen, in the sense that the effect of the collar was to reduce the extracted electron current, without increasing the negative ion current.

Experiments with a stainless steel grid.

Following the report [6, 7] that a negatively biased stainless steel grid placed in front of the plasma electrode could enhance the negative ion production in an ECR source, we also introduced a large stainless steel grid (0.55 mm wire diameter, 2 mm gap) in Camembert III, at 5 cm from the plasma electrode. No improvement was obtained by the presence of the grid and its negative polarization. This is a demonstration of the fact that in our device the microwaves are completely absorbed before reaching the grid and no energetic electrons are produced near this grid.

CONCLUSION.

The elementary ECR sources appear to be useful components for a future negative ion source. The studied network of seven sources produced at a distance of about 10 cm from them a plasma with optimum electron temperature for negative ion production, not much affected by wall effects. The extractor location should be optimized in order to take advantage of the properties of this plasma.

We can note that the pressure affects differently the plasma characteristics, measured near the ECR sources at distance d, and the extracted currents, measured at larger distances D, where d = D – 15 cm. The negative ion density increases monotonously with pressure, up to 4 mTorr, while the extracted current measured 15 cm farther, attains a maximum at 1.5 mTorr.

It seams that we deal with two different regimes at distance range 5 – 10 cm (where probe measurements are made) and at distance range 19.5 – 24.5 cm (where extracted currents are studied).

In the first regime we observe direct negative ion formation in the plasma flowing from the EC sources, with the characteristic effect of electron temperature, enhancement of negative ion density with gas density and weak wall effect.

In the second regime a gas pillow interferes with this process, limiting the optimum pressure to 1.5 mTorr and leading to a strong wall effect.

ACKNOWLEDGEMENT.

The support of European Community (Contract No. HPRI-CT-2001-50021) is gratefully acknowledged.

REFERENCES

1. G. Hellbloom, C. Jacquot, N.I.M. **A243**, 255 (1986)
2. M. Mozjetchkov, T. Takanashi, Y. Oka, K. Tsumori, M. Osakabe, O. Kaneko, Y. Takeiri, T. Kuroda, Rev. Sci. Instrum., **69**, 971-973 (1998)
3. K. Hashimoto, S. Asano, Fusion Eng. Design, **26**, 495 (1995)
4. C.I. Ciubotariu, Thèse de Docteur en Sciences de l'Université Paris XI Orsay (1997) Orsay No. 4793
5. M. Tanaka, K. Amemiya, Rev. Sci. Instrum., **71**, 1125-1127 (2000)

6. R.J. Gobin, O. Delferrière, R. Ferdinant, F. Harrault, K. Benmeziane, G. Gousste, J.D. Sherman, Rev. Sci. Instrum., **75**, 1741 (2004)
7. K. Benmeziane, Thèse de Docteur en Sciences de l'Université Paris XI Orsay (2004)
8. A. Lacoste, T. Lagarde, S. Béchu, Y. Arnal and J. Pelletier, Plasma Sources Sci. Technol. **11**, 407-412, 2002
9. C. Courteille, A.M. Bruneteau, M. Bacal, Rev. Sci. Instrum. **66**, 2533 (1995)
10. A.A. Ivanov, Jr., C. Rouillé, M. Bacal, Y. Arnal, S. Béchu, J. Pelletier, Rev. Sci. Instrum., **75**, 1750-1753 (2004)
11. J. Peters, Rev. Sci. Instrum. **69**, 992 (1998)
12. K.N. Leung, C.A. Hauck, W.B. Kunkel, S.R. Walter, Rev. Sci. Instrum., **61**, 1110 (1990)
13. M. Bacal, J. Bruneteau, P. Devynck, Rev. Sci. Instrum., **59**, 10 (1988)
14. M. Bacal, Rev. Sci. Instrum., **71**, 3981-4006 (2000)
15. M. Bacal, A.A. Ivanov Jr, C. Rouillé, M. Nishiura, M. Sasao, Proceedings of the 30th EPS Conference on Controlled Fusion and Plasma Physics, July 7-11, 2003, St. Petersbourg, Russia
16. A.A. Ivanov Jr, Rev. Sci. Instrum., **75**, 1754-1756 (2004)
17. Microwave Excited Plasmas, Plasma Technology, vol. 4, edited by M. Moisan and J. Pelletier (Elsevier, Amsterdam, 1992), Chap. 10-12.
18. M. Bacal, A.A. Ivanov Jr., M. Glass-Maujean, Y. Matsumoto and M. Nishiura, M. Sasao, M. Wada, Rev. Sci. Instrum., **75**, 1699 (2004)